COMMUNICATION

Synthesis of Porous Bi_2WO_6 Thin Films as Efficient Visible-Light-Active Photocatalysts

By *Li-Wu Zhang, Ya-Jun Wang, Han-Yun Cheng, Wen-Qing Yao,* and *Yong-Fa Zhu**

Heterogeneous photocatalysts offer great potential for converting photon energy into chemical energy and for decomposing organic contaminants.[1] Typical examples are TiO_2-based photocatalytic detoxification of air and water for environmental remediation.[2] However, the band gap of TiO_2 is larger than 3.0 eV, which means it can only show activity under UV irradiation. Thus, the commercialization of this technology has been hindered.[3] Anion-doping with N, C, and S or cation-doping with transition metals are commonly used to functionalize TiO_2 as a visible-light photocatalyst.[4] However, these doped TiO_2 materials show low absorption of visible light; moreover, their photocatalytic activities are still very low, due to complicated factors. The development of efficient visible-light-active photocatalysts has been an urgent issue from the viewpoint of using solar energy.

Pioneering work done by Zou et al.[5] displayed water-splitting for H_2 and O_2 evolution in a stoichiometric amount over the $NiO_x/In_{0.9}Ni_{0.1}TaO_4$ photocatalyst under visible-light irradiation. Following this work, many new visible-active catalysts have been reported, such as Bi_2WO_6,[6] $BiVO_4$,[7] $CaBi_2O_4$,[8] and $InVO_4$.[9] These new ternary metal oxide semiconductors show great potential in the utilization of solar energy.

These photocatalysts are usually utilized as suspended powders. However, the limitation of the low photocatalytic efficiency and the laborious recollection of the powders have considerably restricted their applications. In order to overcome the obstacles, porous TiO_2 films on solid supports have been developed.[10] Porous TiO_2 materials exhibit a large specific surface area, high porosity, and excellent photocatalytic performace. Unfortunately, to the best of our knowledge, there are still no reports focused on the highly porous films of visible-light-active ternary metal oxide photocatalysts.

In this communication, we describe a strategy for extending the general methodology of template-directed synthesis to the formation of porous ternary metal oxides. We present for the first time a simple and reproducible route to ordered porous Bi_2WO_6 films with open pores, as an example of a photocatalytically active ternary metal oxide under visible-light irradiation. The photocatalytic activity of the as-prepared porous films was evaluated by the decomposition of methylene blue (MB) under visible light ($\lambda > 420$ nm) irradiation: ordered porous Bi_2WO_6 films exhibited a much higher photocatalytic activity and photocurrent coversion efficiency than nonporous Bi_2WO_6 films.

Scheme 1 outlines the typical synthesis of ordered porous Bi_2WO_6 films. The preparation is performed by combining evaporation-induced self-assembly and the amorphous complex-precursor method. By using surfactants, block copolymers, or colloid spheres as the templates, porous sigle-phase oxide films have been obtained by hydrolysis of metal alkoxides, such as SiO_2, TiO_2, ZrO_2, and so on.[11] From the viewpoint of developing an economical, preferentially solution-based route to porous ternary metal oxide films, in the current work an amorphous complex precursor was prepared and utilized instead of the metal alkoxide. The homogenous amorphous complex precursor was produced by complexation between diethylenetriaminepenta-acetic acid and the low-cost metal oxide or salt. The high viscosity of the precursor renders it suitable for preparation of the complex oxide films, by dip-coating or spin-coating techniques. Monodisperse carbon spheres with sizes of about 300 nm and 400 nm were synthesized according to a reported procedure,[12] and a packed carbon-sphere monolayer was generated on an indium tin oxide (ITO) glass by vertical deposition[13] of the carbon spheres in ethanol. The spin-coating infiltration method was employed to achieve a homogeneous infiltration of the precursor. Finally, the cabon spheres were eliminated from the film by heating in air.

Figure 1 shows the scanning electron microscopy (SEM) images of the carbon-sphere-monolayer array and porous Bi_2WO_6 film synthesized with different sizes of carbon spheres and different concentrations of precursor. The ordered monolayer structure of the carbon-spheres array is evidenced from the SEM image in Figure 1a. The layer was composed of an hexagonal array of carbon spheres with diameters of 340 nm. Cracks were observed in the array; Koh and Wong[14] have pointed out that the occurrence these is due to the disappearance of the Debye screening layers. The disappearance of Debye screening layers resulted in high stresses on the array, and the response for this

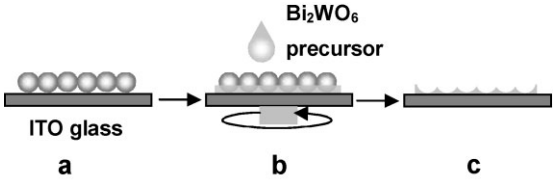

Scheme 1. Schematic illustration of the preparation of the ordered porous Bi_2WO_6 films: a) a packed carbon-sphere monolayer on ITO glass; b) infiltration of the Bi_2WO_6 precursor by spin-coating; c) removal of the carbon spheres by heating in air.

[*] Prof. Y.-F. Zhu, Dr. L.-W. Zhang, Y.-J. Wang, H.-Y. Cheng, W.-Q. Yao
Department of Chemistry, Tsinghua University
Beijing, 100084 (PR China)
E-mail: zhuyf@mail.tsinghua.edu.cn

DOI: 10.1002/adma.200801354

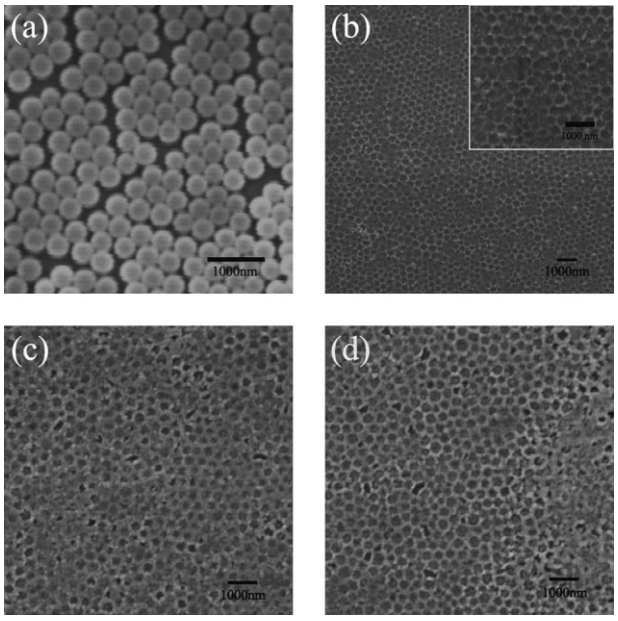

Figure 1. SEM images of: a) the ordered monolayer structure of the carbon spheres; b) a porous Bi_2WO_6 film synthesized with 340 nm carbon spheres and 0.05 g mL^{-1} Bi_2WO_6 precursor; c) a porous Bi_2WO_6 film synthesized with 340 nm carbon spheres and 0.1 g mL^{-1} Bi_2WO_6 precursor; and d) a porous Bi_2WO_6 film synthesized with 390 nm carbon spheres and 0.1 g mL^{-1} Bi_2WO_6 precursor.

effect inevitably causes cracking. Figure 1b–d shows the SEM images of the as-prepared porous Bi_2WO_6 films. The porous Bi_2WO_6 films in Figure 1b and c were synthesized with the same diameter of carbon spheres (340 nm), but with different complex-precursor concentrations. When the concentration of precursor was lower, part of the framework of the porous structure was disconnected (Figure 1b). As the concentration of the precursor increased, the completeness of the frameworks of the porous structure increased (Figure 1c). Moreover, the thickness of the porous walls also increased with the precursor concentration increasing. The porous Bi_2WO_6 films in Figure 1c and 1d were synthesized with the same concentration of the complex precursor, while carbon spheres with a diameter of 390 nm were utilized in the case shown in Figure 1d. The average size of the open pores increased from 290 nm to 320 nm as the diameter of the carbon-sphere template increased. All of the samples underwent shrinkage of the pores during calcination. As noted from the SEM images, the thickness of the Bi_2WO_6 walls could be adjusted by changing the concentration of Bi_2WO_6-complex precursor. Furthermore, we can readily adjust the size of the pores by changing the diameter of the carbon spheres, which could be easily realized by changing the hydrothermal temperature or time.

Figure 2A shows the X-ray diffraction (XRD) patterns of porous and nonporous Bi_2WO_6-film electrodes. The peaks could be well assigned to orthorhombic Bi_2WO_6, while signals from the ITO substrate were also detected, due to the thin films obtained in the present work. The thickness of the film was roughly evaluated to be about 60 nm from the cross-sectional SEM observations. Raman spectra of the as-prepared samples are shown in Figure 2B. The peaks in the range 600–1000 cm^{-1} are assigned

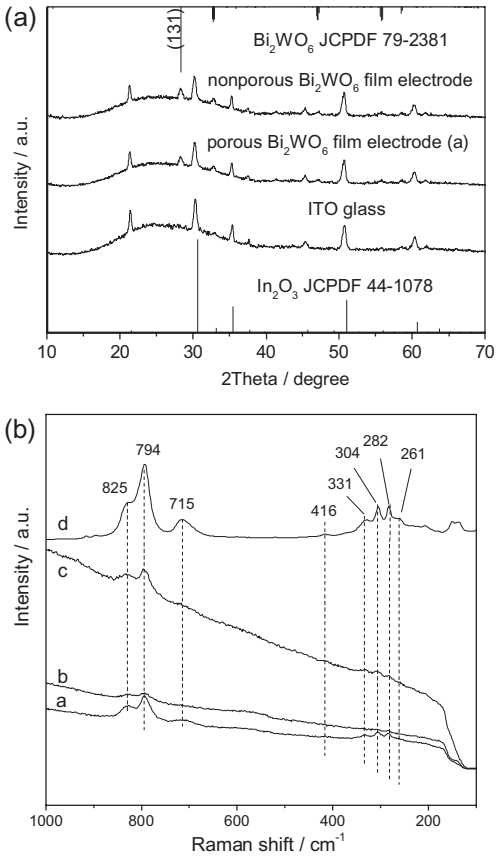

Figure 2. A) XRD patterns of porous and nonporous Bi_2WO_6 film electrodes. B) Raman spectra of: a) a porous Bi_2WO_6 film synthesized with 340 nm carbon spheres and 0.1 g mL^{-1} Bi_2WO_6 precursor; b) a porous Bi_2WO_6 film synthesized with 340 nm carbon spheres and 0.05 g mL^{-1} Bi_2WO_6 precursor; c) a porous Bi_2WO_6 film synthesized with 390 nm carbon spheres and 0.1 g mL^{-1} Bi_2WO_6 precursor; and d) the Bi_2WO_6 powder, for comparison.

to the stretching of the W–O bands, according to a report by Crane et al.[15] In more detail, the bands at 790 and 820 cm^{-1} are associated with the antisymmetric and symmetric A_g modes of terminal O–W–O groups. The band at 310 cm^{-1} can be assigned to translational modes involving simultaneous motions of Bi^{3+} and WO_6^{6-}. The intensity of the peak at 700 cm^{-1} is interpreted as an antisymmetric bridging mode, associated with the tungstate chain. As can be seen, an increased precursor concentration is connected with an enhancement of the intensities of the bands. The result confirmed the formation of a Bi_2WO_6 crystal phase in the porous films.

The photodegradation of methylene blue (MB) was tested as a model reaction to evaluate the photocatalytic activity of the samples. As a comparison, we also prepared a nonporous Bi_2WO_6 film. Figure 3 shows $\ln(C/C_0)$ as a function of time under visible-light ($\lambda > 420$ nm) irradiation, where C is the concentration of MB at the irradiation time t and C_0 is the concentration in the adsorption equilibrium of the photocatalysts before irradiation. A first-order linear relationship was revealed by the plots of $\ln(C/C_0)$ versus irradiation time. Via the first-order linear fit, the determined reaction-rate constants, k, were 0.0019 and 0.0039 min^{-1}, respectively, for nonporous and porous Bi_2WO_6

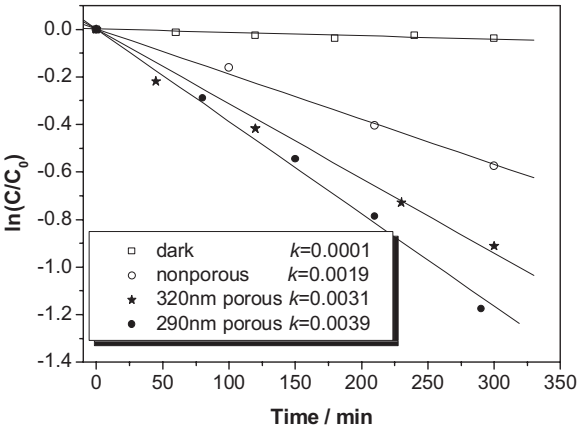

Figure 3. Photodegradation of MB in the presence of porous Bi_2WO_6 films with pore sizes of 290 nm and 320 nm under visible-light irradiation. The nonporous film was studied for comparison.

films with pore sizes of 290 nm. The photocatalytic decomposition rate over the porous film was more than twice as fast as the nonporous sample. The porous Bi_2WO_6 film with the larger pore size (320 nm) showed a slightly lower activity ($k = 0.0031$ min^{-1}) than the 290 nm pore-sized sample, but it was still much more active than the nonporous film. A dark experiment (without irradiation) was also performed, in which the MB decomposition was negligible.

The photo-electrochemical properties of the porous Bi_2WO_6 film (290 nm pore size) were also investigated. Figure 4a shows potentiodynamic scans (10 mV s^{-1}) under chopped illumination for porous and nonporous Bi_2WO_6 films. The electrolyte was a Na_2SO_4 aqueous solution without additive. The anodic photocurrent was observed at more than the open-circuit potential ($V_{op} = -0.10$ V), and the photocurrent increased steadily with the applied positive potential. It is evident that an enhanced photocurrent is obtained essentially over the entire potential range for the porous Bi_2WO_6 film. In particular, for both films, the photocurrent increased more or less linearly as the potential rose from −0.1 to 1.0 V. It is interesting to note that there was a fivefold difference in the slope (photocurrent vs. potential) between the two films. The slope corresponds to the inverse resistance of contact between the working electrode material and the electrolyte.[16] In the case of the porous Bi_2WO_6 film, the resistance was lower, so the photocurrent increased rapidly with the applied potential. In fact, the slope is strongly related to the texture of the film. In the case of the porous Bi_2WO_6 film, due to the much larger electrolyte area exposed, a much larger part of the structure is affected by the field of the Schottky junction at the semiconductor electrolyte interface. Thus, the drift of photogenerated carriers within the width of the Schottky space charge layer becomes a key factor of the porous structure. Attributed to the much smaller distance from the place the charge carriers were generated in the Bi_2WO_6 to the interface between the Bi_2WO_6 and the electrolyte solution, the efficiency of the charge-carrier transportation was higher in the porous Bi_2WO_6 film than in the nonporous film, and an effective separation of the charge carriers could be anticipated. The photogenerated-charge-separation process on the porous and nonporous Bi_2WO_6 films was further investigated by electrochemical impedance spectroscopy (EIS).

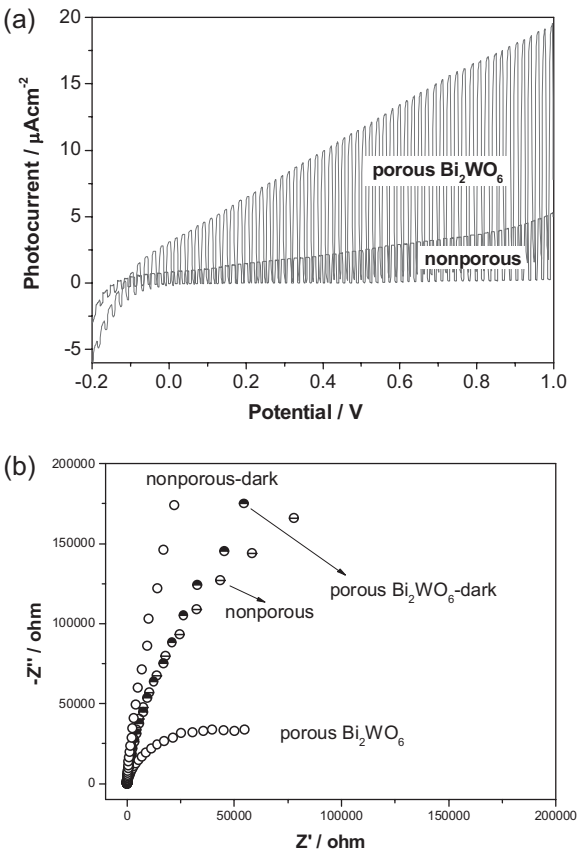

Figure 4. a) Potentiodynamic scans under chopped illumination for porous and nonporous Bi_2WO_6 films, and b) the EIS response of porous and nonporous Bi_2WO_6 films under visible-light irradiation ($\lambda > 420$ nm).

Figure 4b shows the EIS response of porous and nonporous Bi_2WO_6 films under visible-light irradiation ($\lambda > 420$ nm). The radius of the arc on the EIS Nyquist plot reflects the reaction rate occurring at the surface of electrode. The arc radius on the EIS Nyquist plot of the porous Bi_2WO_6 film is smaller than that of the nonporous Bi_2WO_6 film, indicating an effective separation of photogenerated electron-hole pairs, and that fast interfacial charge transfer to the electron donor/electron acceptor occurred, as suggested by Leng et al.[17]

The photocurrent action spectra were also measured. The results for both the porous and nonporous Bi_2WO_6 film electrodes are shown in Figure 5. The electrode of the porous Bi_2WO_6 film showed a maximum photocurrent at 340 nm, located in the UV range. Interestingly, the electrode of the porous Bi_2WO_6 film showed a broad photocurrent peak with a higher intensity, covering the range of 320–460 nm. The fivefold enhancement of the photocurrent conversion in the range of 320–460 nm shows the superiority of the porous Bi_2WO_6 film in light utilization and photocatalysis.

The stability of the porous Bi_2WO_6 film was also studied. The as-prepared samples, as a type of film, can be easily recycled. The photodegradation of MB was tested as a model reaction. The photocatalytic activity did not decrease after five successive cycles of degradation tests, indicating that the porous Bi_2WO_6 film is fairly stable under the studied conditions.

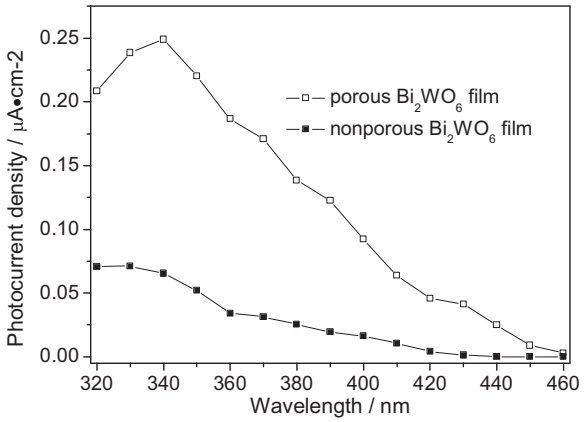

Figure 5. Action spectra of porous and nonporous Bi_2WO_6 film electrodes.

In conclusion, we have demonstrated an economic and reproducible method of preparing porous complex ternary metal oxide semiconductor films of, for example, Bi_2WO_6, with a high photocatalytic activity in the visible-light range. In comparison to the corresponding nonporous Bi_2WO_6 films, the porous films offer a highly enhanced photocatalytic activity under illumination with visible light. The porous film also showed much higher photocurrent conversion efficiency over a wide range of applied potentials. This paper provides a promising route for the improvement of solar-energy utilization.

Experimental

Synthesis of Ordered Porous Bi_2WO_6 Films: Firstly, monodisperse carbon spheres about 300 nm and 400 nm in size were synthesized according to the reported procedure [12]. Briefly, glucose was dissolved in water (40 mL) to form a clear solution, which was placed in a 40 mL teflon-sealed autoclave and maintained at 160 °C for 4 h. The resulting carbon spheres were isolated and washed. The ordered carbon-sphere-array template was prepared by an established vertical-deposition technique. A glass slide was held vertically in a 10 mL vial containing an ethanol suspension of the obtained monodisperse carbon spheres (1%). As the ethanol evaporated and the meniscus swept down the substrate, capillary forces induced ordering of the spheres on both sides of the ITO glass slide.

The amorphous complex precursor used for the infiltration of the void volume of the formed carbon-sphere monolayer was produced as follows: 0.02 mol of diethylenetriaminepenta-acetic acid (H_5DTPA) and 7.5 mL of stronger ammonia water (about 13.0 mol L^{-1}) were added to 200 mL of hot distilled water. After dissolution, 0.005 mol of Bi_2O_3 powder and 0.005 mol of $5(NH_4)_2O \cdot 12WO_3 \cdot 5H_2O$ powder were added. The solution was stirred and heated to about 80 °C to promote the dissolution and reaction (complexation of Bi^{3+} and W^{6+} with DTPA), until the mixture became a colorless transparent solution. To achieve a homogeneous infiltration of the obtained porous precursor, the spin-coating infiltration method was employed in our case. As in a standard spin-coating process, a drop of the precursor (30 mL) was dropped onto the carbon-sphere-packed monolayer, while spinning at a high speed of 60 rps. The film was then allowed to cure in an oven at 70 °C for two days, in order to increase the connectivity of the porous network. Finally, the used templates and the organic components in the precursor were eliminated by heating in air at 500 °C.

Synthesis of Bi_2WO_6 Nonporous Films: A drop of the amorphous complex precursor (30 mL) was dropped onto an ITO glass slide while spinning at a high speed of 60 rps. Then, the film was allowed to cure in an oven at 70 °C for two days, and the organic components in the precursor were eliminated by heating in air at 500 °C.

Photochemical Experiments: The optical system for the photocatalytic reaction was composed of a 500 W Xe arc lamp and a cutoff filter ($\lambda > 420$ nm). The average light intensity was 31 mW cm^{-2}. In a typical process, a solution of MB (usually 10 mL, 1×10^{-5} M) and Bi_2WO_6 film were placed in a vessel. Prior to irradiation, the solution was put in the dark for ca. 30 min, to ensure the equilibrium of the working solution. The solution was kept under constant air-equilibrated conditions before and during the irradiation. The pH value of the reaction suspension was not adjusted. At given time intervals, 3 mL aliquots were sampled and analyzed by recording the variations of the absorption-band maximum in the UV-vis spectra of the dyes, using a Hitachi U-3010 spectrometer.

Photo-electrochemical measurements were carried out using a conventional three-electrode, single-compartment glass cell fitted with a synthesized quartz window using a potentiostat. The quartz electrolytic cell was filled with 0.1 M Na_2SO_4. The Bi_2WO_6 film electrode served as the working electrode. The counter and reference electrodes were a platinum-black wire and saturated calomel electrode (SCE), respectively. The photo-electrochemical experiment was performed using an electrochemical system (CHI-660B, PR China).

Analysis Techniques: X-ray diffraction (XRD) experiments were carried out using a Rigaku DMAX-2400 diffractometer with Cu Kα radiation. The morphology of the Bi_2WO_6 film was characterized using a JSM 6301 electron scanning microscope (SEM). The cross-sectional SEM research was performed for a rough evaluation of the film thickness. Raman spectra were acquired uing a Raman microspectrometer (Renishaw 1000 NR) using an Ar ion laser (514nm). The Raman spectra were measured under a microscope using a 20 × objective to focus the incident excitation laser radiation into a spot 1–2 μm or 2–3 μm in diameter to collect the scattered light. The laser power was kept low enough to avoid heating of the samples, by optical filtering and/or defocusing of the laser beam at the sample surface. Spectra were collected in the range of 1000–200 cm^{-1} with a resolution of 1 cm^{-1}.

Acknowledgements

This work was partly supported by the Chinese National Science Foundation (20673065) and the National Basic Research Program of China (2007CB613303). Supporting Information is available online from Wiley InterScience or from the author.

Received: May 16, 2008
Revised: July 17, 2008
Published online: December 16, 2008

[1] a) M. A. Fox, M.T. Dulay, *Chem. Rev.* **1993**, *93*, 341. b) O. Legrini, E. Oliveros, A.M. Braun, *Chem. Rev.* **1993**, *93*, 671.
[2] A. Fujishima, K. Honda, *Nature* **1972**, *238*, 37.
[3] a) M. Addamo, V. Augugliaro, A. DiPaola, E. Garcia-Lopez, V. Loddo, G. Marci, R. Molinari, L. Palmisano, M. Schiavello, *J. Phys. Chem. B* **2004**, *108*, 3303. b) H. Kominami, S. Murakami, J. Kato, Y. Kera, B. Ohtani, *J. Phys. Chem. B* **2002**, *106*, 10501. c) J.C. Yu, L. Zhang, Z. Zheng, J. Zhao, *Chem. Mater.* **2003**, *15*, 2280.
[4] a) R. Asahi, T. Morikawa, T. Ohwaki, K. Aoki, Y. Taga, *Science* **2001**, *293*, 269. b) S. U. M. Khan, M. Al-Shahry, W.B. Ingler, *Science* **2002**, *297*, 2243. c) B. Kraeutler, A.J. Bard, *J. Am. Chem. Soc.* **1978**, *100*, 4317. d) H. K. Shanmugasundaram Sakthivel, *Angew. Chem. Int. Ed.* **2003**, *42*, 4908.
[5] Z. G. Zou, J. H. Ye, K. Sayama, H. Arakawa, *Nature* **2001**, *414*, 625.
[6] a) H. B. Fu, C. S. Pan, W. Q. Yao, Y. F. Zhu, *J. Phys. Chem. B* **2005**, *109*, 22432. b) J. W. Tang, Z. G. Zou, J. H. Ye, *Catal. Lett.* **2004**, *92*, 53. c) C. Zhang, Y.F. Zhu, *Chem. Mater.* **2005**, *17*, 3537. d) L.S. Zhang, W.Z.

Wang, L. Zhou, H. L. Xu, *Small* **2007**, *3*, 1618. e) A. Kudo, S. Hijii, *Chem. Lett.* **1999**, 1103.

[7] a) A. Kudo, K. Ueda, H. Kato, I. Mikami, *Catal. Lett.* **1998**, *53*, 229. b) K. Sayama, A. Nomura, T. Arai, T. Sugita, R. Abe, M. Yanagida, T. Oi, Y. Iwasaki, Y. Abe, H. Sugihara, *J. Phys. Chem. B* **2006**, *110*, 11352. c) S. Tokunaga, H. Kato, A. Kudo, *Chem. Mater.* **2001**, *13*, 4624. d) J.Q. Yu, A. Kudo, *Adv. Funct. Mater.* **2006**, *16*, 2163.

[8] J. W. Tang, Z. G. Zou, J. H. Ye, *Angew. Chem. Int. Ed.* **2004**, *43*, 4463.

[9] a) J. H. Ye, Z. G. Zou, M. Oshikiri, A. Matsushita, M. Shimoda, M. Imai, T. Shishido, *Chem. Phys. Lett.* **2002**, *356*, 221. b) L. W. Zhang, H. B. Fu, C. Zhang, Y. F. Zhu, *J. Solid State Chem.* **2006**, *179*, 804.

[10] a) L. Zhang, Y. F. Zhu, Y. He, W. Li, H. B. Sun, *Appl. Catal. B* **2003**, *40*, 287. b) M. Zukalova, A. Zukal, L. Kavan, M. K. Nazeeruddin, P. Liska, M. Gratzel, *Nano Lett.* **2005**, *5*, 1789. c) J. H. Pan, W. I. Lee, *Chem. Mater.* **2006**, *18*, 847.

[11] a) C. J. Brinker, Y. F. Lu, A. Sellinger, H. Y. Fan, *Adv. Mater.* **1999**, *11*, 579. b) P. D. Yang, D. Y. Zhao, D. I. Margolese, B. F. Chmelka, G. D. Stucky, *Chem. Mater.* **1999**, *11*, 2813. c) H. S. Yun, K. Miyazawa, H. S. Zhou, I. Honma, M. Kuwabara, *Adv. Mater.* **2001**, *13*, 1377.

[12] a) X. M. Sun, Y. D. Li, *Angew. Chem. Int. Ed.* **2004**, *43*, 597. b) X. M. Sun, Y. D. Li, *Angew. Chem. Int. Ed.* **2004**, *43*, 3827.

[13] P. Jiang, J.F. Bertone, K. S. Hwang, V. L. Colvin, *Chem. Mater.* **1999**, *11*, 2132.

[14] Y. K. Koh, C. C. Wong, *Langmuir* **2006**, *22*, 897.

[15] M. Crane, R. Frost, P. Williams, T. Kloprogge, *J. Raman Spectrosc.* **2002**, *33*, 62.

[16] B. Yang, Y. J. Zhang, E. Drabarek, P. R. F. Barnes, V. Luca, *Chem. Mater.* **2007**, *19*, 5664.

[17] W. H. Leng, Z. Zhang, J. Q. Zhang, C. N. Cao, *J. Phys. Chem. B,* **2005,** *109*, 15008.